Scanning tunneling microscopy observations on the reconstructed Au(111) surface: Atomic structure, long-range superstructure, rotational domains, and surface defects

J. V. Barth, H. Brune, and G. Ertl
Fritz-Haber-Institut der Max-Planck-Gesellschaft, Faradayweg 4-6, D-1000 Berlin 33, West Germany

R. J. Behm
Institut für Kristallographie und Mineralogie, Universität München, Theresienstrasse 41, D-8000 München 2, West Germany

(Received 18 April 1990)

High-resolution scanning tunneling microscopy data on the reconstructed Au(111) surface are presented that give a comprehensive picture of the atomic structure, the long-range ordering, and the interaction between reconstruction and surface defects in the reconstructed surface. On the basis of the atomically resolved structure, the stacking-fault-domain model involving periodic transitions from fcc to hcp stacking of top-layer atoms is confirmed. The practically uniform contraction in the surface layer along $[1\bar{1}0]$ indicates that the previously proposed soliton functionalisms are not correct descriptions for the fcc→hcp stacking transition. The lateral displacement of ~0.9 Å in the $\begin{pmatrix} 22 & 0 \\ \bar{1} & 2 \end{pmatrix}$ unit cell along $[11\bar{2}]$ is in good agreement with the transition between fcc and hcp stacking. The vertical displacement in the transition regions (0.20±0.05 Å) is largely independent of the tunneling parameters, while the atomic corrugation (0.2 Å typically, up to 1 Å) depends strongly on tunneling parameters and tip conditions. The two different stacking regions within the unit cell are directly identified from the domain pattern at step edges; fcc stacking is deduced for the wider areas and thus is energetically more favorable. A new long-range superstructure is reported. It is created by a correlated periodic bending of the parallel corrugation lines by ±120° every 250 Å, i.e., rotational domains are arranged in a zigzag pattern. Interactions on this scale indicate long-range elastic lattice strain. This structure reflects the overall tendency to isotropic contraction, combining the locally favorable uniaxial contraction and an effective isotropic contraction on a larger scale. Boundaries of rotational domains can also be formed by a termination of the reconstruction lines. Individual corrugation lines, separating different stacking regions, cannot disappear. The termination occurs in well-ordered, U-shaped connections of neighbored lines or by a complicated pattern of entangled corrugation lines. Steps and bulk defects do not inhibit the reconstruction, but can affect the local reconstruction pattern. In most cases steps are crossed by the reconstruction lines, and the strict correlation of the reconstruction pattern on the terraces, both in phase and orientation, reflects interaction over the step edge. Sometimes the reconstruction pattern at the steps resembles those found at rotational domain boundaries.

I. INTRODUCTION

Gold is the only fcc metal that exhibits a reconstruction of the close-packed (111) surface. This has been observed by means of low-energy electron diffraction (LEED),[1–3] reflection high-energy electron diffraction (RHEED),[4] transmission electron microscopy (TEM),[5–7] helium atom scattering (HAS),[8] and, most recently, scanning tunneling microscopy (STM).[9] The electron diffraction pattern was interpreted in terms of a superstructure with a local, twofold symmetry, which due to the higher, threefold symmetry of the fcc(111) surface exists in three rotational domains.[4] An analysis of the LEED satellite pattern led to the proposition of a one-dimensional domain superstructure with nonequivalent domain pairs, i.e., pairwise-arranged domain boundaries.[2] The authors proposed a domain system created by periodically arranged regions with stacking faults and partial dislocations of the (compressed) topmost-layer atoms in the transition regions between bulk site (fcc) atoms and hcp atoms. At the same time and also based on LEED studies, a model involving a uniaxial and uniform contraction of the topmost hexagonal layer along $[1\bar{1}0]$, leading to a rectangular unit cell with lattice vectors $22a$ and $\sqrt{3}a$, was suggested.[3]

The TEM photographs of small, epitaxially grown Au(111) platelets, "fringes" of about 63-Å spacing were seen, which independently led to the proposal of a domain structure with fcc- and hcp-type stacking regions. In this model the contraction of the surface is localized in narrow transition regions.[7] Based on their He diffraction data, Harten *et al.* confirmed and further improved the above stacking-fault-domain model.[8] They allowed the transition regions from fcc to hcp stacking to be more extensive and modeled them by "Frenkel-Kontorova"-type solitons[10] with a half-width of 11.8 Å and a vertical corrugation of 0.15 Å. The latter was described by a Gaussian. Different relative sizes were evaluated for fcc and hcp domains.[8] This feature cannot be deduced from the Frenkel-Kontorova model,[11] but found a natural explana-

tion in a theoretical approach, where a "double-sine-Gordon" potential was introduced, taking explicitly into account the energetic nondegeneracy of fcc and hcp sites.[12] In a recent STM study the different relative widths of the domains and the lateral displacements of the topmost-layer Au atoms normal to the contraction direction became directly visible.[9]

In contrast to the above soliton models a theoretical study of the Au(111) reconstruction, based on the "embedded-atom" formalism, came to the conclusion of a nearly uniform shrinking of the surface along $[1\bar{1}0]$ with wide transition regions separating fcc and hcp domains.[13] However, the authors could not reproduce the correct size of the unit cell. The decision on the question of uniform versus localized compression relies on the ability to determine the exact positions of the Au atoms within the $\begin{pmatrix} 22 & 0 \\ -1 & 2 \end{pmatrix}$ unit cell which has not been possible so far. Furthermore the tentative assignment of fcc and hcp stacking to the respective two regions is not yet confirmed.

The topmost, reconstructed Au layer is expected to still exhibit significant internal strain, resulting from the uniaxial rather than isotropic contraction. It will be shown that this strain leads to a specific long-range ordering of rotational domains in the reconstructed layer. Local defects can also be expected to sensitively affect the reconstruction pattern in the surface layer and these effects may allow conclusions on the strain fields in the surface.

These various aspects of the Au(111) reconstruction are the subject of the present scanning tunneling microscopy study. We have investigated the character of the surface contraction by analyzing STM images that resolve both the reconstruction pattern and the atomic positions. Due to the local nature of the STM, this technique is particularly well suited for the investigation of the local effects described above. Rotational domains were identified and structural details of the domain boundaries were examined. The interaction between atomic steps as well as other surface defects and the reconstruction was analyzed. The reconstruction pattern at step edges allowed a direct assignment of fcc and hcp stacking regions.

II. EXPERIMENT

The experiments were performed under ultrahigh-vacuum (UHV) conditions, using a "pocket-sized" STM with a vertical stability better than 0.02 Å.[14,15] Standard techniques such as Ar-ion bombardment, LEED, and Auger spectroscopy were available for *in situ* preparation and analysis of the surface. The Au(111) single crystal was prepared by cycles of Ar sputtering (2 μA, 500 V, 30 min) and annealing (900 K) until no contaminations could be detected by Auger spectroscopy. The tunneling tip was electrochemically etched from polycrystalline W wire (0.7 mm diameter). Prior to the STM measurements it was cleaned by field desorption in front of a gold foil. It was then brought into a high-resolution state by applying short bias pulses of up to -9 V to the sample potential during tunneling. This method is identical to that used for tip preparation applied for atomic resolution imaging on Al(111) and presumably leads to mass transport from the sample to the tip.[14,15] Atomic resolution was reliably achieved this way. All STM images were acquired in the "slow scan" mode, at constant tunnel current. They typically consist of 270×270 data points. No filtering procedures were applied for the data shown here.

III. RESULTS

The topography of the clean and well-annealed Au(111) surface is characterized by large, atomically flat terraces, which often extend over many hundred ångstroms. They are separated mostly by monoatomic steps of $\sim$2.4 Å height as shown in the STM image in Fig. 1. This image also demonstrates the variety of different shapes found on this surface. In addition to extended linear steps, which were predominantly oriented along close-packed lattice directions such as $[1\bar{1}0]$, also round or irregular steps with a high density of kinks were frequently observed. There is a slight preference for close-packed steps in low-index directions, but this is not at all as pronounced as for other close-packed surfaces such as Pt(111) or Ru(0001),[16–18] where straight steps were found to extend over 1000 Å or more and the kink density was very low.

The terraces exhibit a periodic pattern of pairwise-arranged, parallel lines, running in $[11\bar{2}]$ direction (corrugation lines), as can be seen in Fig. 2. The distance between neighbored pairs—in $[1\bar{1}0]$ direction—amounts to 63 Å; the individual lines within a pair are about 44 Å apart. The corrugation amplitude of 0.20 ± 0.05 Å was found to be largely independent of the tunneling parameters and tip conditions. The depression of the narrow re-

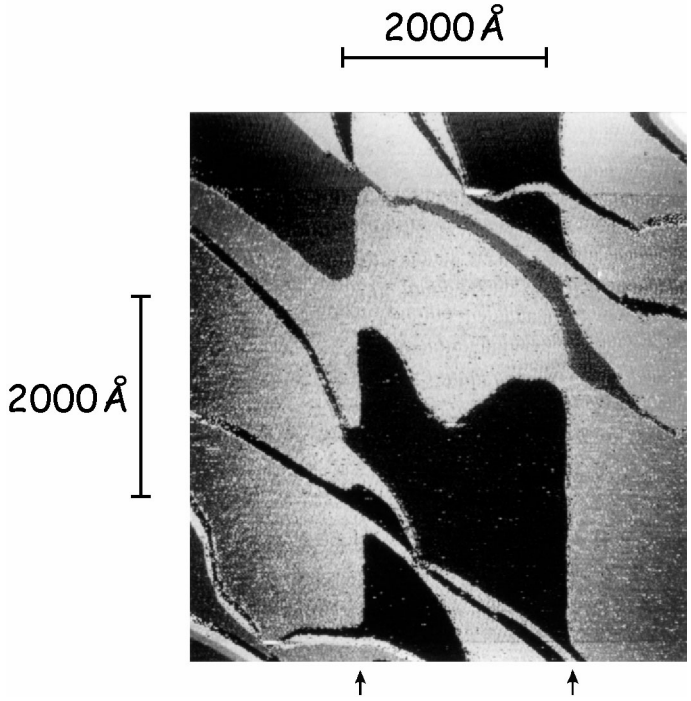

FIG. 1. Step-terrace topography of a well-prepared, reconstructed Au(111) surface (5000×5000 Å^2); consecutive terraces are shaded dark and light. Note the parallel steps in y direction indicated by an arrow are cutting through all other steps.

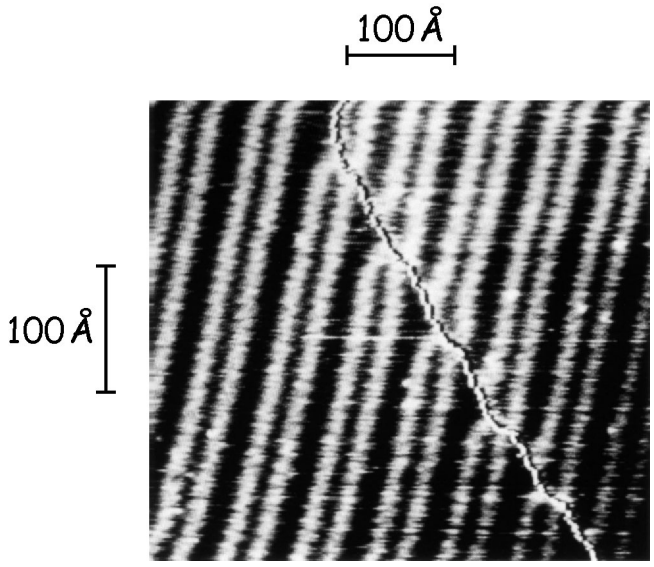

FIG. 2. Pairwise-arranged corrugation lines on the reconstructed Au(111) surface (450×450 Å^2); vertical corrugation amplitude 0.2 Å. A monoatomic step passes diagonally through the image, it is crossed by the reconstruction.

gions between the two lines of each pair is less pronounced ($\sim 0.12 \pm 0.05$ Å). Patterns of this type with a slightly smaller corrugation amplitude of 0.15 Å were reported already in a recent STM study by Wöll *et al.*[9] and associated with the reconstruction of the surface. These authors had shown that the corrugation pattern of the STM image is very similar to the corrugation pattern derived from He diffraction,[8] confirming the reconstruction model proposed in the latter work.

High-resolution STM images of the surface such as the one presented in Fig. 3 reveal an additional, more dense corrugation, superimposed over the long-wave corrugation of the reconstruction. From the hexagonal arrangement of the minima and the distance of 2.7 to 2.9 Å between neighboring minima, these are attributed to the atomic structure of the surface. Thus the individual metal atoms are resolved in the STM image, as was demonstrated first for this surface by Hallmark *et al.*[19]

Surprisingly in many cases the minima rather than the maxima in the STM images reflect the hexagonal arrangement of the surface atoms. Although the mechanism governing resolution of individual atoms on close-packed metal surfaces remains to be fully clarified, it is conceivable that under certain conditions the atoms are imaged as minima rather than as maxima or vice versa.[20,21] This possibility is, however, disproved by Fig. 4, which demonstrates that these differences result rather from resolution effects in the STM measurements. In this image the tip undergoes an abrupt change while scanning, which leads to a sudden vertical jump of the tip by about 0.5 Å closer to the surface in the upper third of the image. Therefore the sample surface appears deeper by an equivalent amount in the lower part of the image. In the upper part of the image the hexagonal arrangement of atomic lattice is reproduced by the minima while in the lower part of the image it is reflected by the maxima. Nevertheless maxima and minima are exactly aligned in both parts of the image. Consequently the surface atoms always relate to the maxima (or the minima) in both parts of the image; i.e., this does not depend on the tip condition. But apparently certain tip states or tip geometries can affect the resolution of the STM measurement in such a way that in one case all threefold hollows are represented as minima (maxima)—leading to a hexagonal arrangement of the maxima (minima) in the STM image—while in the other case only one type of threefold hollows is imaged as a minimum (maximum) and these minima (maxima) show up as a hexagonal pattern.

The measured atomic corrugation depends strongly on the tunneling conditions. Using the tip preparation technique described above, amplitudes up to ~ 1 Å were observed at low tunnel resistances, i.e., tunnel currents up to ~ 600 nA. Similarly to a recent STM study on Al(111),[14,15] an exponential decay of the corrugation amplitude was found over several angstroms variation in the

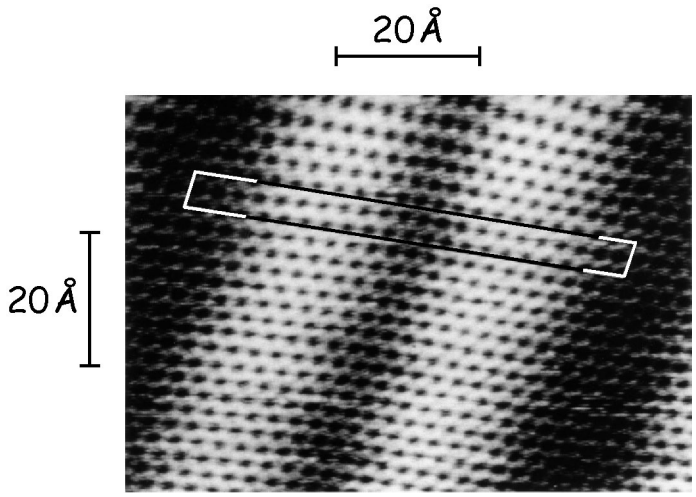

FIG. 3. Atomic resolution STM image of the reconstructed Au(111) stretching over two pairs of corrugation lines (white); the unit cell is marked in the figure (atomic corrugation 0.2 Å; $I_t = 631$ nA, $V_t = -69$ mV).

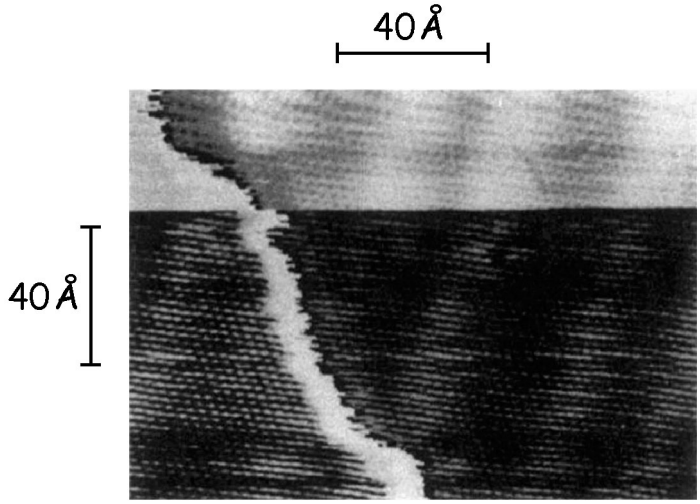

FIG. 4. Au(111) topograph taken while a change in the tip state reversed the resolution, the lower part of the image appears at an ~ 0.5-Å lower level as a result. A monoatomic step crosses at the left side, the two terraces are colored individually.

tip surface separation. In the same range the tunnel current also decayed exponentially; typical values for the tunnel barrier ranged between 2 and 3.5 eV, but values as low as 0.5 eV were also found occasionally. Even in the vicinity of steps, atomic resolution could be achieved, although these tunneling conditions often led to significant modifications in the tip (cf. Fig. 4) and subsequent loss of the high lateral resolution.

Atomic resolution images of the surface allow a direct and simple determination of the unit cell of the reconstructed layer, which is marked by a rectangle in Fig. 3. The lattice vectors are given by the connection between adjacent main minima, 63 Å in the $[1\bar{1}0]$ direction, and by the connection between next-neighbor $[1\bar{1}0]$ rows of Au atoms, 4.7 Å in the $[11\bar{2}]$ direction, respectively. This leads to a $\begin{pmatrix} 22 & 0 \\ \bar{1} & 2 \end{pmatrix}$ unit cell, compatible with previous results.[1–9] Also, by comparison of atomic rows in $[1\bar{1}0]$ with the lines marking the unit cell the lateral displacement of the surface atoms along $[11\bar{2}]$, normal to the contraction direction, becomes directly apparent. It is determined to ~0.9 Å, equivalent to the $\sqrt{3}/6a$ distance betwee fcc and hcp sites expected from a hard-sphere model (0.83 Å).

A detailed evaluation of the atomic positions within the unit cell, averaging over many atomic rows in several STM images comparable to the one in Fig. 3, gives further information on the structure of the reconstructed surface. The spacing between adjacent atoms in $[1\bar{1}0]$, as a function of the position along $[1\bar{1}0]$ within the unit cell, is plotted in Fig. 5. The observation of 23 Au surface atoms per unit cell, on 22 bulk lattice sites, is consistent with the calculated average contraction of 4.55%. The plot in Fig. 5 shows that the contraction of the atomic distances is not confined to the transition regions. Rather the distance between neighboring Au atoms shows an oscillatory behavior with an amplitude of about 0.1 Å around the constant value for a uniformly contracted layer (2.75 Å). Within the limits of accuracy there are no regions of preferential contraction; if present at all, they appear to be concentrated in the fcc and hcp rather than in the transition regions. The structural implications of this result will be discussed below.

Three different rotational domains were observed. They often coexist on a single terrace, especially on larger

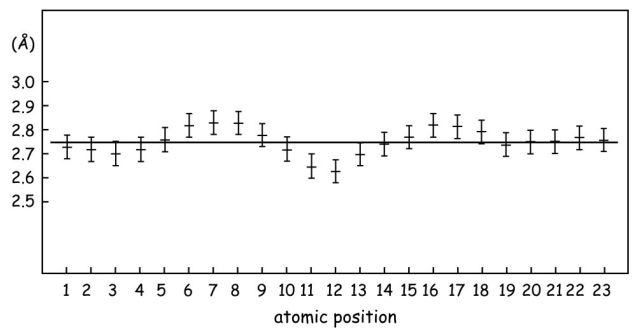

FIG. 5. Plot of the distance—in $[1\bar{1}0]$ direction—between atomic rows in $[11\bar{2}]$ direction as a function of the atomic position along $[1\bar{1}0]$ in the unit cell marked in Fig. 3 (row 1 is located at the left corner of the unit cell).

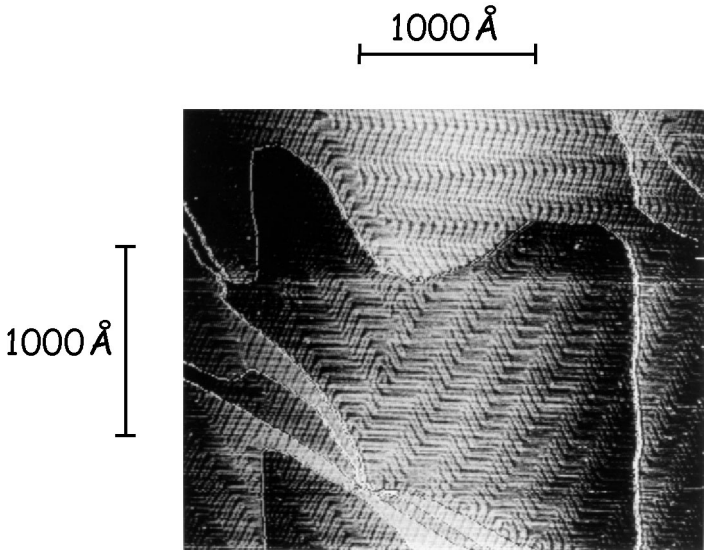

FIG. 6. Overview showing a large surface area with a regular arrangement of domain boundaries created by a zigzag pattern (±120°) of the reconstruction (distance between domain boundaries approximately 250 Å).

ones. In most cases the transition from one domain into another one occurs by a correlated bending of the corrugation lines by 120°. Usually an additional long-range periodicity in the reconstructed layer is observed. Entire sets of corrugation lines change their orientation in a zigzag pattern by ±120° and thus form a periodic sequence of domain boundaries. An example for this kind of super periodicity is reproduced in Fig. 6. The distance between domain boundaries amounts to about 250 Å. Interactions between domain boundaries on this scale can only be rationalized in terms of long-range lattice strain.

A more detailed inspection of the (rotational) domain boundaries in Fig. 7 reveals that the corrugation line

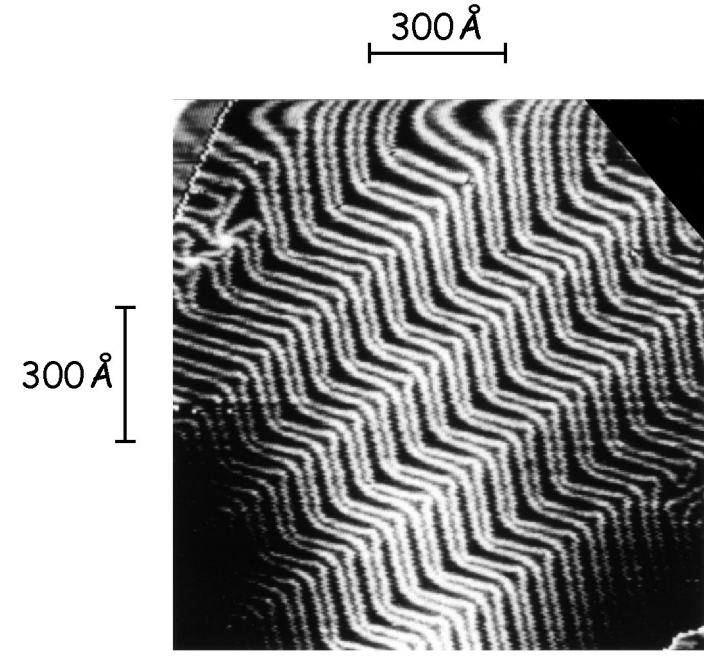

FIG. 7. Detailed image of periodic rotational domains in the reconstructed surface as shown in Fig. 6. Note the nonparallel arrangement of the corrugation lines at the bending points.

pairs are characteristically deformed in the vicinity of the bending points, i.e., near the domain boundaries. The distance between the lines is either increased or decreased, but they never bend exactly parallel. In addition the corrugation amplitude of the reconstruction is often increased in this area. Another interesting feature is found in the upper left edge of Fig. 7, where six corrugation lines meet in a single point leading to a local threefold symmetry of the reconstructed surface.[22]

The presence of domain boundaries does not necessarily correspond to a well-ordered zigzag arrangement of the corrugation lines like the patterns in Figs. 6 and 7. In the following STM image (Fig. 8) the corrugation lines collectively change their direction by 120° every 200 Å on average, but this time all three orientations are present and a rather complicated pattern of entangled lines is formed. Another novel feature in this image is presented by the U-shaped connections between neighboring corrugation lines. These U's can connect either both lines in a pair or lines of adjacent pairs, as visible in the upper right corner. A U connection of neighboring lines corresponds to the termination of either a fcc or a hcp region at this position. In this image the corrugation lines again do not run parallel in the vicinity of the bending points.

Even more disordered domain boundaries were observed occasionally. Since they appeared only on rather small terraces and thus seemed to be related to the presence of atomic steps they will be described below.

So far the minima between the corrugation lines were associated with fcc and hcp stacking regions, respectively. If this is correct, then the two types of U connections cannot exist in the direct neighborhood, since the areas surrounding the respective U termination correspond to different stacking regions. Adjacent U connections of different type must be separated by an additional transition region equivalent to a single corrugation line in between. This conclusion is confirmed by the STM image

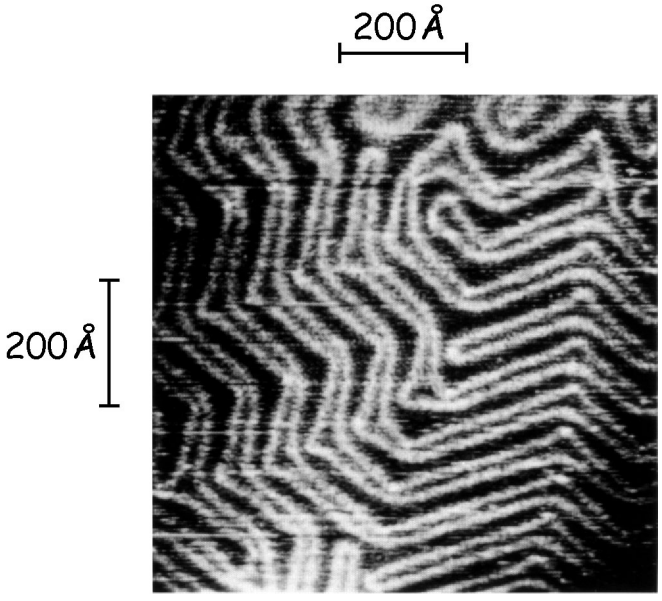

FIG. 8. Surface area with many small rotational domains; the corrugation line pairs exhibit the same, nonparallel arrangement in the bending points as shown in Fig. 7.

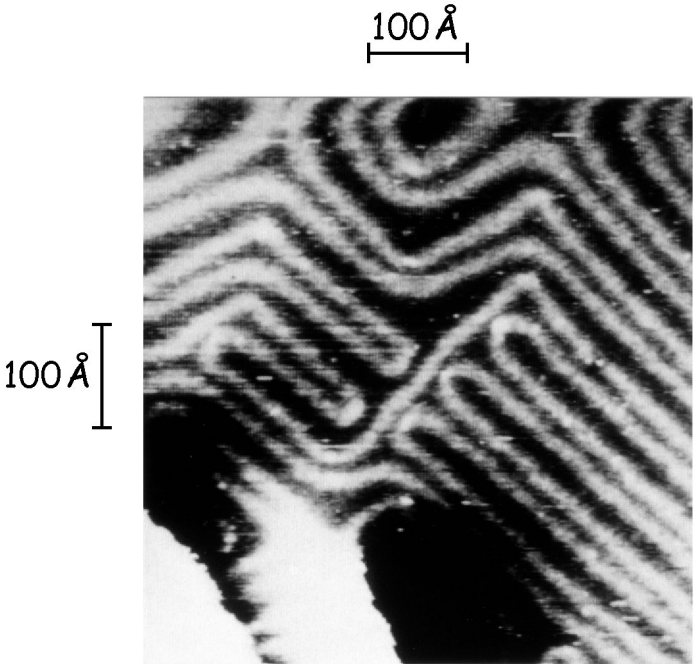

FIG. 9. U-shaped connections of two adjacent corrugation lines, terminating a line pair. Connections occur either between lines of one pair or between lines of two neighboring pairs.

in Fig. 9, where both types of U connections are present. In the left-hand side the lines of individual pairs are connected, while for the lines coming from the lower right corner the connection is made between lines of neighboring pairs, i.e., in the first case the narrow regions and in the second the wide regions are terminated by the U-

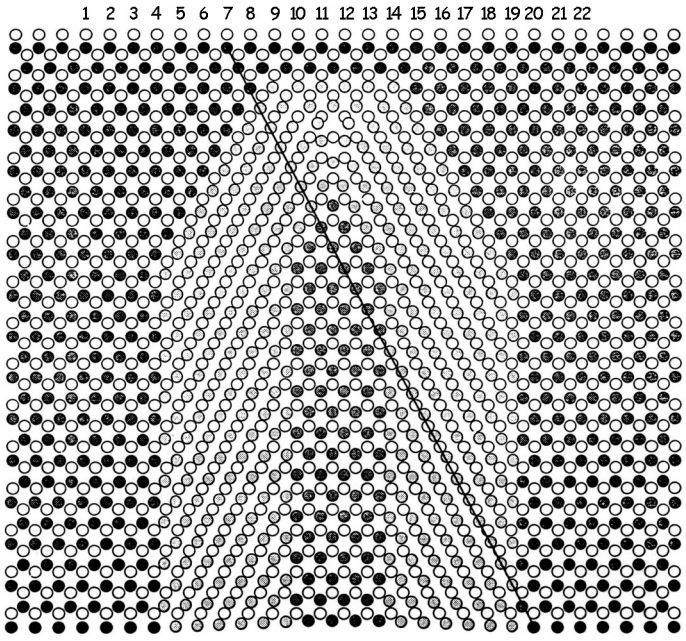

FIG. 10. Model of the atomic structure of a U connection between two corrugation lines (Fig. 11); open circles, atoms of the second layer; dashed circles, atoms of the top layer (dark, fcc domain; light, transition region, medium, hcp region). The dark line marks a cut along the surface atoms passing through two transition regions. This line and thus the surface atoms are rotated by ~2° with respect to the substrate lattice.

shaped connections. The two types of U connections are indeed separated by another line marking a transition region, in perfect agreement with the above conclusions. This single line does not follow the usual $[11\bar{2}]$ direction, but runs orthogonal in $[1\bar{1}0]$ direction. Remarkably, its width and amplitude are similar to the usual values, which points to a similar structural origin of that line. In fact, this transition region can easily be modeled by a sequence of unit-cell halves, which are displaced by one atom in $[1\bar{1}0]$ with respect to each other.

The domain model has stringent implications for the arrangement of surface atoms in the region of a U connection. This is illustrated in a schematic model in Fig. 10. In the ordered, reconstructed surface additional Au atoms are inserted in the contraction direction. This cannot be the case in the region right outside the U connection, where no transition region exists. An extra row of Au atoms along $[11\bar{2}]$ thus ends at the apex of the U. Secondly the reconstruction leads to a slight rotation of the close-packed rows of surface Au atoms which form an angle of 30° with the corrugation lines by $\sim 1.5°$ with respect to the bulk lattice. In the regions outside the U connection, however, the reconstruction is locally absent and the topmost Au atoms are oriented along fcc or hcp stacking sites of the second layer. Accordingly those close-packed rows do not run parallel in these two regions and the contraction of the surface has the consequence that an additional atomic row appears in between them on the open side of the U connection. These suggestions are clearly verified in the STM image in Fig. 11 which represents a detail of Fig. 9 and where the atomic structure in the vicinity of a U connection is resolved. In this image four small arrows indicate points with comparable distances in the contraction direction $[1\bar{1}0]$ inside and outside the U. It is easily counted that in the first case there are 19 atoms in between them while in the second one this number is only 18. The rotation of the close-packed rows in $[1\bar{1}0]$ is illustrated by the two straight lines marking such rows of surface atoms, one passing through the U and one lying outside. On the left side of the image these lines are nine atomic distances apart, while on the right-hand side, sideways of the U, this distance is now ten atomic rows. These simple structural considerations provide a direct proof of the contraction of the topmost layer along $[1\bar{1}0]$, without any ambiguities due to calibration errors, etc., and thus further confirm the structural model for the Au(111) reconstruction.

So far we have concentrated on structural details of the reconstruction of an unperturbed Au(111) surface. Because of the long-range strain in the topmost layer accompanying the reconstruction surface defects such as steps are expected to play a major role for the formation and ordering of the reconstruction. But bulk defects such as screw dislocation lines will also introduce strain at the point where they appear at the surface, and may thus interfere with the reconstruction.

All of the line pairs pass through the steps without any apparent lateral displacement or even a change in direction at the step edge. This observation was confirmed in many STM images (Figs. 2 and 6) and is seen as being typical for the reconstruction. This is illustrated again in Fig. 12, which was recorded on a more stepped area covering several terraces. While no additional structure was observed at the step edge in this image, Fig. 2 reveals further details. Slight changes in the line pairs at the step edge are noticed. On the lower terrace the lines are bent inwards; they almost look like U connections located right at the step edge.

Figure 12 also illustrates the impact of another kind of

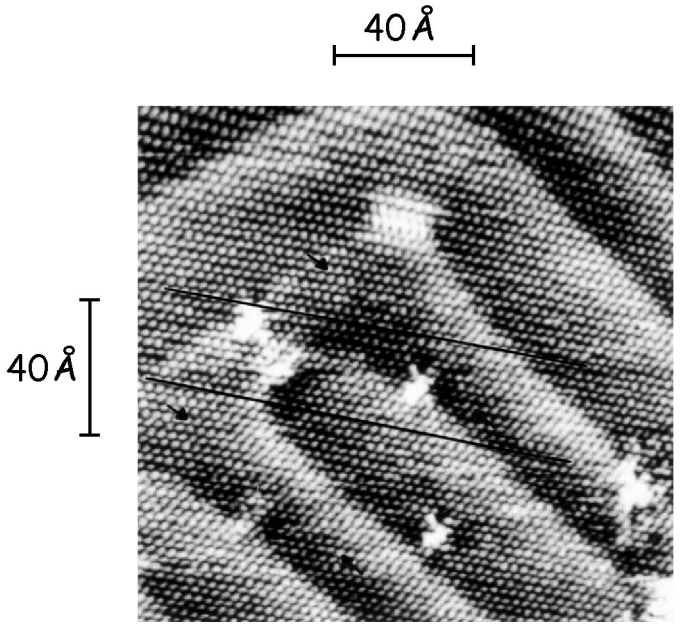

FIG. 11. High-resolution image of the atomic structure in the vicinity of a U connection. The dark lines mark two cuts along atomic rows in the $[1\bar{1}0]$ direction. The lower cut passes through the U connection, the upper one remains outside. At the left side of the U, one less atomic row can be counted in between them than at the right side (9 vs 10). This reveals directly the higher density of surface atoms and thus the contraction in the reconstructed surface with periodic transition regions.

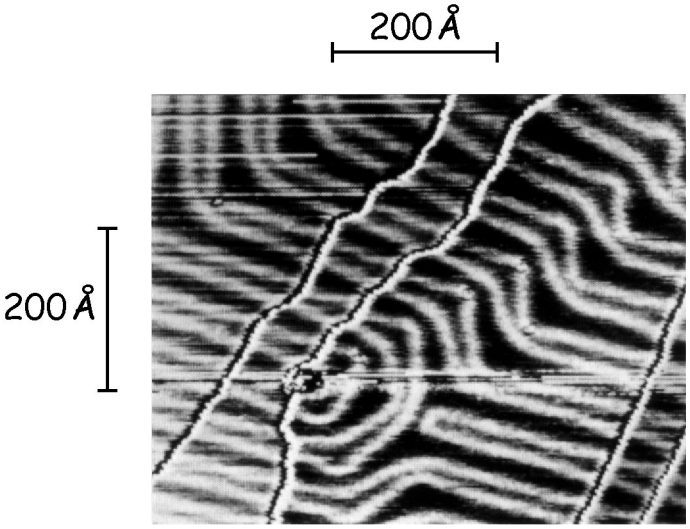

FIG. 12. Interaction between reconstruction and steps (640×520 Å^2). The reconstruction and thus the corrugation lines proceed straight over the steps.

surface defect on the reconstruction. In the left part of the image the surface is further distorted by a hole in the topmost Au layer (~20 Å diameter), right at the step edge. It may be speculated that these holes, which are rarely observed on other metal sufaces, relate to the contraction of the topmost layer during the reconstruction process. This defect causes a long-range modification in the reconstruction pattern. Two parallel line pairs follow the perimeter of the hole from step edge to step edge. All line pairs coming from the right side of the imaged surface area are forced to give way for this area and are displaced sideways, and the central line pair directed at the hole is terminated by a U connection.

In some cases the line pairs are terminated by U connections before they reach the step edge or, especially on rather narrow terraces, the reconstructed layer is not well ordered and the transition regions are arranged in a complicated nonperiodic pattern. This is reproduced in Figs. 13 and 14, respectively. Also in the latter case the shape and amplitude of the corrugation line are comparable to that found on more ordered areas. In the right-hand side of this image a small ordered area with parallel line pairs on the middle terrace is still visible.

The last two figures illustrate another characteristic structural feature. In both of them U connections are observed, which are formed by connecting lines of neighborhood line pairs. These U's are not directly beside the steps, however, but are separated by an additional corrugation line running parallel to the step. A similar single corrugation line was already described above for the case

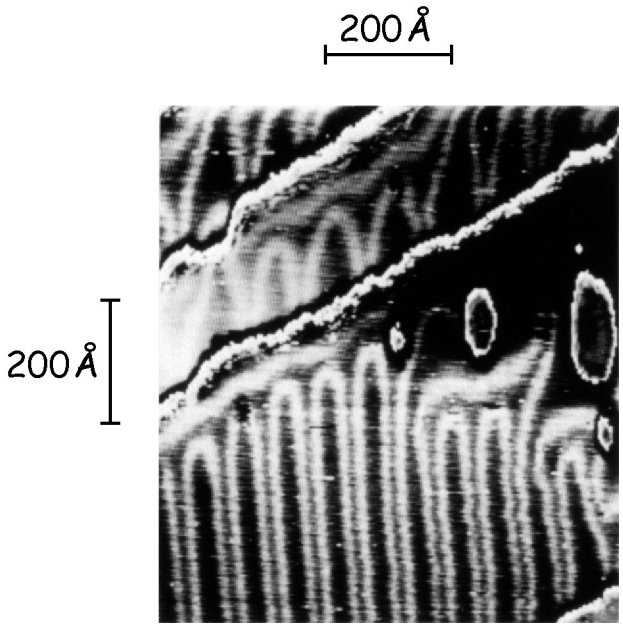

FIG. 13. Interaction between reconstruction and steps on a 700×780 Å^2 surface area. A well-ordered region on the lower terrace is terminated by U connections between lines of neighboring line pairs. The wide (fcc) domains are terminated, the narrow (hcp) domains are left open towards the step. The hcp region is separated from fcc stacking at the step edge by a single corrugation line along the step. The reconstruction pattern is affected by the three holes in the topmost atomic layer at the right-hand side of the image such that the corrugation lines follow the perimeter of the holes.

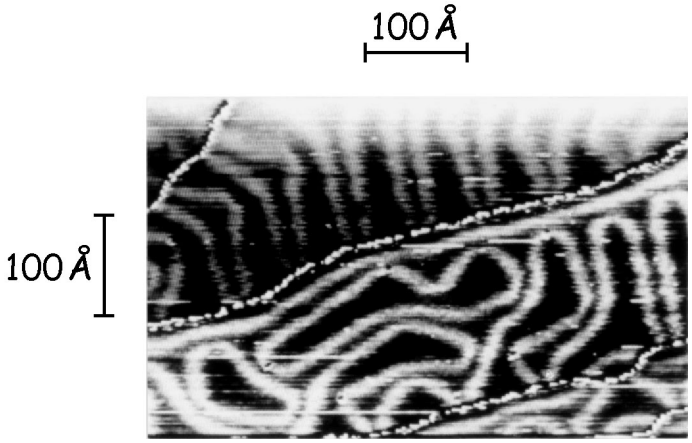

FIG. 14. Interaction between reconstruction and steps on a 520×320 Å^2 surface area. A rather irregular reconstruction pattern is exhibited on the central, narrow terrace, a single corrugation line along the step separates fcc stacking at the step edge from a hcp region (U connections enclose the wide fcc region and leave the hcp region open).

of neighboring U's of different type. Its existence could be explained in terms of the present structural model. The structural change in the surface layer at the step edge in combination with the resolution of different stacking regions allows an unambiguous assignment of the two different regions to fcc and hcp stacking, respectively, which had not been possible so far. This assignment is based on the assumption that the Au atoms in the second layer are located on bulk sites, i.e., on fcc sites. In that case the Au atoms in the topmost, reconstructed layer of the lower terrace adjoin the Au atoms on fcc sites in the second, bulklike layer of the upper terrace. It can be concluded that those Au surface atoms of the lower terrace directly adjacent to step edges reside on fcc sites. Hence the stacking type of the different domains in the STM images in Figs. 13 and 14 can be determined by simple counting. The wider domains in between the stripes are unambiguously identified as fcc regions, and the narrower regions must be hcp domains. It was discussed already by El-Batanouny *et al.*[12] that the different widths of the two domains reflect the difference in energy of the stacking sites. As expected from the bulk lattice, the fcc domain is more favorable.

Bulk defects are generally not accessible by surface sensitive techniques. The situation is different in those cases where the bulk defect emerges at the surface. This is demonstrated in Fig. 15. In the center of the STM image a vertical screw dislocation ends at the surface. Following the model in Fig. 16(a) an emerging screw dislocation line is identified on the surface by the sudden onset of a step in the middle of a flat terrace. A similar structure is observed in Fig. 15(a); in fact in this case two steps emerge from that point, indicating a twofold screw dislocation. The interaction with the reconstruction is more clearly visible in the top-view representation of the same STM image in Fig. 15(b). It shows that the corrugation lines bend towards the dislocation center in the surrounding area. From these images one can conclude that the surface strain caused by emerging screw dislocations does

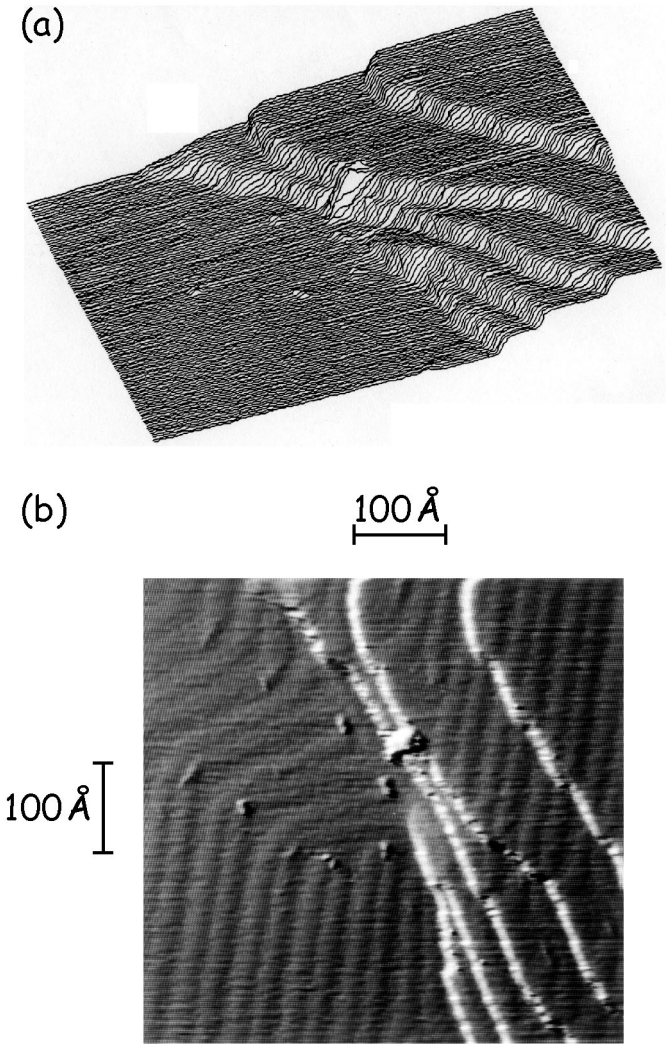

FIG. 15. Image of an area with a screw dislocation line emerging at the surface (550×490 Å^2). (a) Three-dimensional line-scan representation showing the formation of two steps on the lower terrace; (b) top-view representation of the same emphasizing the reconstruction pattern in the bottom terrace.

not inhibit the reconstruction, but it does affect the reconstruction pattern. The strain fields induced by screw dislocations and by normal steps insofar have similar effects on the reconstruction.

Screw dislocations were observed rather frequently on this surface, in contrast to our experience on other materials such as Al,[14,15] Pt,[16] or Ru.[17,18] Nevertheless their density is still very low and hence these kinds of bulk defects cannot be investigated by integrating surface techniques. Again the STM is a unique tool in this respect.

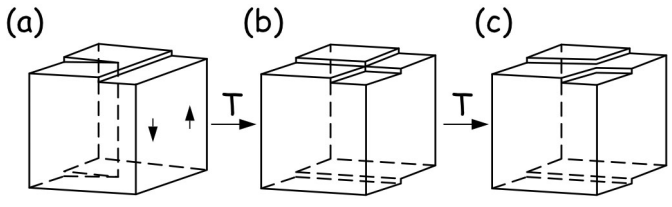

FIG. 16. Formation of intersecting steps upon removal of a screw dislocation (schematic description). (a) Surface with vertical screw dislocation line; (b) the same area after removal of the screw dislocation; (c) connection of terraces on equal levels by surface diffusion.

In the absence of screw dislocations the step-terrace arrangements follows the large scale topography of the surface, with steps proceeding mostly normal to the overall inclination. Removal of a screw dislocation, e.g., by annealing, results in a slipping of the bulk material along a plane ending at the dislocation line by one atomic layer, as indicated in Fig. 16.[23] In that case a new surface step is created which proceeds over the surface along the trace of the slip plane. The resulting step is independent of the existing step-terrace structure; steps in other directions are crossed [Fig. 16(b)]. This mechanism explains the formation of intersecting surface steps as observed occasionally [cf. Fig. 15(a)]. This effect had been demonstrated previously by Bethge *et al.* for different materials by scanning electron microscopy (SEM) imaging.[23] The same authors had shown that diffusion processes, e.g., induced by further annealing after the dislocation had been removed, lead to a characteristic modification of the area directly surrounding the crossing point of two steps. As indicated in Fig. 16(c) the topmost terrace retracts and the bottom terrace is filled up, such that a bridging connection between the two opposite terraces on the same level is created. The surface area imaged in Fig. 1 provides a good example for this phenomenon. Two parallel steps, approximately 2000 Å apart, extend linearly in y direction over the entire surface area, and intersect a number of steps on the surface. The rearrangement at the crossing points as described above is clearly visible; in some cases (in the center of the image) the "connection" between diagonal terraces has a width of up to several hundred angstroms.

IV. DISCUSSION

The STM images of the reconstructed Au(111) surface presented in the preceding section provide a comprehensive picture of the atomic structure, long-range ordering, and interaction between reconstruction and surface defects. The data confirm the general concept and many details of the stacking-fault-domain model by direct imaging of the atomic structure; in addition they demonstrate the existence of long-range elastic strain in the reconstructed layer.

The reconstruction corresponds to the formation of parallel corrugation lines along $[11\bar{2}]$. This corrugation pattern has been described in detail by Wöll *et al.*[9] The lines were interpreted as transition regions between fcc and hcp stacking domains. These authors also noticed that the shape of the STM corrugation is closely related to that of the potential for He scattering derived previously from a fit to experimental intensities.[8] This agrees well with results from model calculations on STM imaging of metal surfaces by Tersoff and Hamann which predict that a spherical tip follows a line of constant charge density at its center.[24] In a first-order approximation the He scattering potential equally follows such contour lines, however, at a rather close distance to the surface.[25]

A $\begin{pmatrix} 22 & 0 \\ \bar{1} & 2 \end{pmatrix}$ unit cell—63×4.7 Å^2—was reproduced in our measurements with 23 atoms on 22 hollow sites along

the [1$\bar{1}$0] contraction direction. The total vertical corrugation of 0.20±0.05 Å, measured between the deeper, wide minima (fcc regions) and the maxima (transition regions), agrees well with previous STM and He diffraction data.[8,9] The narrow minima (hcp domain) are found to be more shallow; at least part of the difference of 0.08 Å with respect to the deep minima may reflect the energetic difference of the diverse stacking sites. The relative widths of the two domains, measured from maximum to maximum in the transition regions, were determined to be 44:19, again in good agreement with previous findings.

In the stacking-fault-domain model the corrugation, i.e., the vertical displacements of the surface atoms within the unit cell, results from the different binding sites of the topmost-layer Au atoms. Threefold-hollow sites are occupied in the fcc and hcp regions in contrast to quasibridge sites in the transition regions. Long-wave corrugations of similar origin were reported also for other reconstructed metal surfaces, namely, the "hex" reconstructed (100) surfaces of Au (Ref. 26) and Pt.[27] On those surfaces a hexagonal topmost layer resides on a square substrate. The corrugation amplitudes (0.3 Å) are comparable to those found on Au(111); the somewhat larger value in the former cases may relate to the fact that on the (100) surfaces the quasibridge sites are forced to move closer to on-top sites.[28]

The measured atomic corrugation depends strongly on tip conditions and tunneling parameters. The exponential decay of the corrugation with increasing tip-surface separation for a given tip resembles recent findings for Al(111).[15] As mentioned already by Wintterlin *et al.*,[15] the observation of an atomic corrugation on these close-packed metal surfaces cannot be understood in the framework of the Tersoff-Hamann description.[24] The maximum values of the corrugation amplitude around 1 Å were obtained under conditions where the tip is very close to the surface. The tip-surface distance in a typical atomic resolution image presented above can be estimated to be approximately 3.5 Å from the preset tunneling resistance (110 kΩ), the measured effective tunnel barrier (2.5 eV), and an estimated resistance at point contact conditions around 30 kΩ.[29] Under these conditions strong interactions between tip and surface have to be anticipated[20,21,30] and were experimentally verified.[31] These interactions are likely also to affect the effective tunnel barrier. Similar values, however, were observed also for larger gap resistances.

The atomic resolution images allow a precise determination of the lateral position of the Au atoms within the $\begin{pmatrix} 22 & 0 \\ \bar{1} & 2 \end{pmatrix}$ unit cell. The interatomic spacings along the [1$\bar{1}$0] contraction direction, evaluated from averaging over several atomic resolution images, however, contrasts with expectations from the previously proposed soliton models,[8,12] since the contraction is not confined to the two transition regions. Hence these models are not considered to provide the correct description for the fcc→hcp stacking transition of the top-layer atoms in the reconstructed Au(111) surface. Concerning this point our results are in better agreement with the recent "glue-model" calculations by Bartolini *et al.*[13]

The contraction of the reconstructed layer is not only apparent by the vertical and lateral displacements of the atoms normal to the contraction direction, but became directly visible from comparing atomic densities across and beside two transition regions at a U termination of the corrugation lines. An additional row of surface atoms was observed in the latter case for passing over the two transition regions, in excellent agreement with the above model.

The STM images presented here provide clear evidence that the reconstruction extends right to the step edges, i.e., there is no stabilization of the unreconstructed phase along the step. This agrees well with STM observations on the "hex" reconstructed Pt(100) surface, where the reconstruction likewise reached up to the step edges.[27] On W(100), by contrast, the reconstruction was reported to be inhibited in regions along step edges.[32]

The different hollow-site domains were directly identified from STM images by evaluating the domain structure along step edges. Assuming that the Au atoms in the topmost layer of the lower terrace reside on the (bulklike) fcc sites directly adjacent to the step edge, the wider regions represent domains with fcc stacking and the narrower ones hcp domains. The obvious energetic preference for fcc stacking agrees well with the fcc bulk structure of Au.

Especially on less well prepared surfaces or, occasionally, on smaller terraces, irregular or poorly ordered reconstruction patterns are observed. Under such conditions the reconstruction may even be totally absent. In a nonlocal reconstruction involving long-range lattice strain such as in the present case this is easily understood in a picture where surface defects can act as pinning centers for the topmost layer and thus inhibit the reconstruction. The increasing degree of order with annealing time reflects the existence of an activation barrier for surface ordering. These irregular corrugation lines are comparable in height and width to those of the ordered reconstruction; the local character of the reconstruction thus can be assumed to be identical in both cases.

The three different rotational domains oriented at 120° to each other reflect the threefold symmetry of the fcc(111) substrate. The predominant and most regular way to transform from one domain orientation to another is offered by a correlated bending of the parallel corrugation line pairs. This type of domain boundary exists also on the "ideal" reconstructed surface and is thus seen as the "regular" and most favorable type of a domain boundary. The distortion of the corrugation line pairs at the bending points must be related to the simultaneous change of the contraction direction. In this area local structures similar to that found in the apex of the U connections have to exist in order to accommodate the additional lattice strain. The fact that, depending on the bending direction, the lines are either attracted or repelled can be explained on the basis of symmetry arguments, i.e., on the combined symmetry of substrate and top layer.

Neglecting the nonrepresentative case of disordered domain boundaries, the other type of domain boundary involves the termination of one rotational domain at the boundary which is accomplished by U-shaped connec-

tions of neighboring corrugation lines. (Because of the stacking-fault-domain structure individual corrugation lines, representing transition regions between fcc and hcp stacking, cannot disappear suddenly.) This way all domains of one stacking type are properly terminated and only a single stacking region adjoins the neighboring rotational domain. Both types of connections possible, those between lines in a pair surrounding a hcp area and those between lines of adjacent pairs terminating a fcc domain, were found. In those cases where line pairs of both (stacking) domains are terminated at the (rotational) domain boundary, only similar type connections can exist in the direct vicinity, again in perfect agreement with the structural model. Coexistent connections of different type are separated by a single corrugation line, i.e., a single transition region.

The additional superstructure observed in this work has not been reported so far. It is built up by a periodic sequence of boundaries between two types of rotational domains with the domains arranged in a zigzag pattern. The domain boundaries are typically about 250 Å apart, but this distance can be affected by surface defects, etc. The dimension of this periodic structure by far exceeds that of all ordered surface structures observed until now. This size is above the resolution limit of most diffraction techniques, which also had prevented its detection by such experiments.

This structure requires the presence of interactions which are effective over distances in the range of several hundred angstroms and can only be achieved by elastic lattice strain in the surface layer. Consequently this type of force represents the physical origin of the observed "superstructure." This explanation fits well into our present understanding of the reconstruction. The unilateral contraction relieves lattice strain in one direction. If one assumes that an isotropic contraction would be most favorable if the interface energy to the substrate were neglected, only in the case of unilateral contraction is the lattice strain still present in the other surface directions. The zigzag arrangement of two different rotational domains results in a structure which has contraction components in all three surface directions. The surface thus minimizes its energy by combining the locally favorable, uniaxial contraction with an effectively isotropic contraction on a larger scale. This zigzag pattern is therefore considered to represent the stable configuration of the reconstructed Au(111) surface, and the bending-type boundaries between rotational domains are indeed an integral part of the ideal, reconstructed surface.

The introduction of an atomic step on the flat surface is expected to give an additional tangential stress component[33] which stands in competition to the in-plane surface strain within the terraces. It was noted before that frequently the corrugation lines and thus the reconstruction proceed straight over steps, with the reconstructed phases on both terraces strictly correlated in phase and in orientation. This requires sufficiently strong interactions between the topmost reconstructed layers on both sides of the step, which presumably are mediated by the second layer of the upper terrace. A deformation of subsurface layers was proposed already on the basis of theoretical considerations.[13,34]

The transmission of strain from one terrace to another one can likewise be rationalized in the framework of the stacking-fault-domain model for the reconstruction. If the corrugation lines pass over a step, atoms in the hcp regions of the reconstructed lower terrace have to connect to fcc atoms in the same layer right at the step edge. This necessitates the formation of domain boundaries ("tranistion regions") in the hcp regions along the steps in these cases, i.e., the hcp regions of the lower terrace must be terminated by a U connection right at the step edge. One may speculate that a slight distortion in that layer on the other side of or right at the step edge, caused by the presence of the topmost reconstructed layer in the upper terrace, governs the formation of transition regions at the step edge and thus the arrangement of hcp regions on the lower terrace. In that case the periodicity in the topmost layer of the upper terrace determines, via strain onto the second layer, the arrangement of the transition regions along the step and thereby the phase and orientation of the reconstruction on the lower terrace. This mechanism rules out domain boundaries at step edges, in agreement with experimental observations.

Domain boundaries at the step edge are possible and were observed only if the fcc domain on the lower terrace was terminated by U connections in the same way as described for domain boundaries on terraces. Depending on the type of U connection an additional corrugation line could extend along the step edge in order to properly connect to the fcc stacking at the step edge. The formation of a continuous fcc domain along the step edge as verified in this latter case appears to be energetically more favorable than a sequence of local transition regions at the step edge required for the reconstruction to pass over a step. Nevertheless the predominant observation of the latter combination points to an energetic preference for that structure. Presumably the termination of a domain by U connections, which is necessary always on the lower terrace if a domain boundary is formed at the step edge, is sufficiently unfavorable. Subsequently in the total energy balance the structure with the reconstruction passing over steps is preferred.

If a lower terrace domain is terminated at a step edge the reconstruction can start again on the next-higher terrace at the step with parallel corrugation lines going off from the step edge. In that case there are no additional domain boundaries required along the step edge, since the upper-terrace atoms can be positioned freely.

The interaction between reconstruction and steps can not only modify or even dominate the reconstruction pattern but can conceivably also affect the step shape. A strong stabilization of certain steps had recently been reported for the 1×2 reconstructed (110) surfaces of Au and Pt.[35,36] In that case extended, kink-free steps along the close-packed $[1\bar{1}0]$ directions were observed. This contrasts with the properties of the unreconstructed surface and has to be attributed to a reconstruction induced stabilization of these steps. For the clean Au(111) surface a slight preference for long, linear steps along low-index directions was noticed, but a large fraction of the steps was rather irregular and exhibited a high kink density.

The interaction between steps and reconstruction thus does not lead to a significant stabilization of certain step directions.

The interaction between reconstruction and screw dislocations as an example for a bulk defect led to effects similar to those observed in the case of steps. These defects, which are identified by the formation of a new step at the breakthrough point of the dislocation line at the surface, in the middle of a flat terrace, were observed rather frequently. Also in that case the reconstruction is not inhibited in the vicinity of the center of the dislocation, but the pattern of the reconstruction is altered. This is comparable to the effect of steps on the reconstruction. In both cases the strain field in the topmost layer is affected by the presence of these surface defects.

The reconstruction of Au(111), although unique for clean metals, apparently represents a more general type of surface structure which can also be formed in heteroepitaxial systems if a hexagonal metal adlayer is grown on top of a slightly larger hexagonal substrate. For a Cu adlayer on the hexagonal Ru(0001) substrate a similar structure was found for the second Cu layer, on top of the pseudomorphic first layer.[17,18] In that case the size of the unit cell is reduced to 46 Å, in good agreement with the contraction calculated from the atomic radii of the Ru and Cu bulk lattices. With the opposite case, i.e., when (significantly) larger metallic atoms are placed on a hexagonal substrate, similar type structures are not possible. In that case the adatoms are too large to occupy neighboring rows in $[1\bar{1}0]$ and a (distorted) isotropic expansion is favored instead, as in the case of Pb adlayers.[37] The strength of the lattice strain fields in these stacking-fault-domain structures, however, must depend critically on the respective materials. For Cu/Ru the well-annealed second Cu layer exhibited linear corrugation lines over many hundred, even thousand angstroms, without any intermediate change in the orientation. This means the formation of the additional, long-range superstructure is not favorable for that system, in contrast to the clean Au(111) surface where the lattice strain appears to produce the long-range structure.

Several arguments on the origin of the Au(111) surface reconstruction have been reported.[13,33,38–40] The crucial point seems to be the interaction of *d* and *sp* electronic states at the surface. This is also suggested by the results of first-principles calculations for an isolated Au(100) layer.[41] Charge redistribution is likewise suspected to play an important role in the dispersion curves of surface phonons of noble metals.[39,42]

Another interesting finding is that the Au(111) reconstruction affects the local reactivity of the surface. It was reported that Ag nucleation occurs preferentially on the faulted region of the unit cell,[43] whereas we found upon deposition of small amounts of K on the surface that the Au atoms in the transition regions are the most reactive.

ACKNOWLEDGMENTS

We gratefully acknowledge Dr. J. Wintterlin for extensive and helpful discussions.

[1]J. Perdereau, J. P. Biberian, and G. E. Rhead, J. Phys. F **4**, 798 (1974).
[2]H. Jagodzinski and D. Wolf, Deutsche Forschungsgemeinschaft, Sonderforschungsbereich Report No. 128 (1980–1982) (unpublished).
[3]M. A. van Hove, R. J. Koestner, P. C. Stair, J. P. Biberian, L. L. Kesmodel, I. Bartos, and G. Somorjai, Surf. Sci. **103**, 189 (1981).
[4]H. Melle and E. Menzel, Z. Naturforsch. **33a**, 282 (1978).
[5]J. C. Heyraud and J. J. Metois, Surf. Sci. **100**, 519 (1980).
[6]Y. Tanishiro, H. Kanamori, K. Takayanagi, K. Yagi, and G. Honjo, Surf. Sci. **111**, 395 (1981).
[7]K. Takayanagi and K. Yagi, Trans. Jpn. Inst. Met. **24**, 337 (1983).
[8]U. Harten, A. M. Lahee, J. P. Toennies, and Ch. Wöll, Phys. Rev. Lett. **54**, 2619 (1985).
[9]Ch. Wöll, S. Chiang, R. J. Wilson, and P. H. Lippel, Phys. Rev. B **39**, 7988 (1989).
[10]F. C. Frank and J. H. van der Merwe, Proc. R. Soc. London, Ser. A **198**, 205 (1949).
[11]Y. I. Frenkel and T. Kontorova, Zh. Eksp. Teor. Fiz. **8**, 1340 (1938) or J. Phys. U.S.S.R. **1**, 137 (1939).
[12]M. El-Batanouny, S. Burdick, K. M. Martini, and P. Stancioff, Phys. Rev. Lett. **58**, 2762 (1987).
[13]A. Bartolini, F. Ercolessi, and E. Tosatti, in *The Structure of Surfaces II,* edited by J. F. van der Veen and M. A. van Hove (Springer, Berlin, 1988).
[14]W. Wintterlin, Ph.D. thesis, Freie Universität Berlin, 1989.
[15]J. Wintterlin, J. Wiechers, H. Brune, T. Gritsch, H. Höfer, and R. J. Behm, Phys. Rev. Lett. **62**, 59 (1989).
[16]B. Eisenhut, Dipolma thesis, Universität München, 1988.
[17]G. Pötschke and R. J. Behm (unpublished).
[18]G. Pötschke, Ph.D. thesis, Universität München, 1990.
[19]V. M. Hallmark, S. Chiang, J. F. Rabolt, J. D. Swalen, and R. J. Wilson, Phys. Rev. Lett. **59**, 2879 (1987).
[20]S. Ciraci, in *Basic Concepts and Applications of Scanning Tunneling Microscopy,* edited by H. Rohrer, R. J. Behm, and N. Garcia (Kluwer, Dordrecht, 1990).
[21]G. Doyen, E. Koetter, J. Barth, and D. Drakova, in *Basic Concepts and Applications of Scanning Tunneling Microscopy,* edited by H. Rohrer, R. J. Behm, and N. Garcia (Kluwer, Dordrecht, 1990).
[22]An argument for why the domain walls form a striped structure rather than a triangular lattice can be found in Y. Okwamoto and K. H. Bennemann, Surf. Sci. **186**, 511 (1986).
[23]H. Bethge, M. Krohn, and H. Stenzel, in *Electron Microscopy in Solid State Physics,* edited by H. Bethge and J. Heydenreich (Elsevier, Amsterdam, 1987).
[24]J. Tersoff and D. R. Hamann, Phys. Rev. B **31**, 805 (1985).
[25]N. Esbjerg and J. K. Norskov, Phys. Rev. Lett. **45**, 807 (1980).
[26]G. Binnig, H. Rohrer, Ch. Gerber, and E. Stoll, Surf. Sci. **144**, 321 (1984).
[27]R. J. Behm, W. Hösler, E. Ritter, and G. Binnig, Phys. Rev. Lett. **56**, 228 (1986).

[28]W. Mortiz, Habilitation thesis, Universität Müchen, 1984.
[29]J. K. Gimzewski and R. Möller, Phys. Rev. B **36**, 1284 (1987).
[30]S. Ciraci, A. Baratoff, and I. P. Batra (unpublished).
[31]U. Dürig, O. Züger, and D. W. Pohl, J. Microsc. (Oxford) **152**, 259 (1988); U. Dürig, J. K. Gimzewski, and D. W. Pohl, Phys. Rev. Lett. **57**, 2403 (1986).
[32]M. K. Debe and D. A. King, Surf. Sci. **81**, 193 (1979).
[33]V. Heine and L. D. Marks, Surf. Sci. **165**, 65 (1986).
[34]R. Ravelo and M. El-Batanouny, Phys. Rev. B **40**, 8574 (1989).
[35]T. Gritsch, D. Coulman, G. Ertl, and R. J. Behm (unpublished).
[36]T. Gritsch, Ph.D. thesis, Freie Universität Berlin, 1990.
[37]G. Meyer, M. Michailov, and M. Henzler, Surf. Sci. **202**, 125 (1988).
[38]B. W. Dodson, Phys. Rev. Lett. **60**, 2288 (1988).
[39]C. S. Jayanthi, H. Bilz, W. Kress, and G. Benedek, Phys. Rev. Lett. **59**, 795 (1987).
[40]R. J. Needs and M. Mausfield, J. Phys.: Condensed Matter **1**, 7555 (1989).
[41]N. Takeuchi, C. T. Chan, and K. M. Ho, Phys. Rev. Lett. **63**, 1273 (1989).
[42]V. Bortolani, G. Santoro, U. Harten, and J. P. Toennies, Surf. Sci. **148**, 82 (1984).
[43]M. M. Dovek, C. A. Lang, J. Nogami, and C. F. Quate, Phys. Rev. B **40**, 11 973 (1989).